Selective Multi-Source Domain Adaptation Network for Cross-Subject Motor Imagery Discrimination

Juho Lee*, Jin Woo Choi*, and Sungho Jo

***Abstract*—Discriminating motor imagery with electroencephalogram (EEG)-based brain-computer interface (BCI) poses a challenge as it involves an extensive data acquisition phase that demands a substantial amount of effort from the user. To address this issue, one approach is to use unsupervised domain adaptation, where classification models are constructed using data from multiple subjects, and only the unlabeled data from the target user is used for model calibration. However, since brain patterns from motor imagery vary between individuals, the reliability of each subject must be considered when multiple subjects are used to build the classification model. Thus in this paper, we propose Selective-MDA that performs domain adaptation on each source subject and selectively limits influences based on their domain discrepancies. To evaluate our approach, we assess our results with two public datasets, BCI Competition IV IIa and the Autocalibration and Recurrent Adaptation datasets. We further investigate the effect of source selection by comparing the discrimination performance when different numbers of source domains are selected based on discrepancy measures. Our results demonstrate that Selective-MDA not only integrates multi-source domain adaptation to cross-subject motor imagery discrimination but also highlights the impact of source domain selection when using data from multiple subjects for model training.**

***Index Terms*—brain-computer interface, unsupervised domain adaptation, motor imagery, electroencephalography, neural decoding.**

I. Introduction

BRAIN-computer interfaces (BCIs) provide direct interaction between the human brain and external devices by decoding neural signals into control commands [1]–[5]. As one of the non-invasive methods to acquire real-time signals, electroencephalogram (EEG) is widely measured in BCIs by placing a set of electrodes on the scalp [6]. In the case of motor imagery-based BCI systems which map imagination of different body movements to control modalities, discriminating intentions are possible even without additional stimulus [7]. Unlike other paradigms, such as P300 [8], [9] or steady-state visually evoked potentials (SSVEP) [10], [11], which distinguish evoked responses from the brain caused by visual stimulants, motor imagery utilizes oscillatory neural signals from the user's imagination. As motor imagery of different body movements exhibits a decrease in neural oscillation from different regions within the sensorimotor cortex, spectral and spatial features from brain signals play an important role in motor imagery discrimination [12], [13].

Extraction of discriminant spectral and spatial features from EEG signals has therefore been an essential component for decoding motor imagery with machine learning methods [14]–[16]. One of the representative methods is filter-bank common spatial pattern (FBCSP) [17], which applies multiple common spatial pattern (CSP) algorithms with varying frequency bands. As an extension to the CSP algorithm, which acts as a spatial filter that maximizes discrimination between features, FBCSP uses multiple pre-defined frequency bands to further consider spatial features within different spectral slices. To overcome the usage of such hand-crafted features and to extract more diverse spatial and spectral features, deep learning methods were also explored [18]–[20]. Previous studies have suggested motor imagery classification models by designing an architecture that behaves similarly to machine learning models. For instance, Schirrmeister et al. [21] proposed an end-to-end Shallow convolutional neural network (Shallow ConvNet) model composed of a sequence of convolutional layers indicating spectral and spatial feature extractions inspired by the FBCSP algorithm. Furthermore, Lawhern et al. [22] proposed a convolutional neural network (CNN) model that extracts frequency-specific spatial features and utilizes compact architecture to lessen the number of trainable parameters.

While the aforementioned studies contributed largely to the enhancement of motor imagery discrimination, applying such models alone to BCI applications still faces challenges as they exhibit low accuracies in cross-subject performance [23], [24]. Even though the models may be trained using data from multiple other subjects, variations in brain signals between individuals cause mismatch in data distributions between the source and target domains, resulting in low classification performance for the data from the target subject. Although the ideal cross-subject scenario would involve the model not utilizing any data from the target subject, it is still essential to have a considerable amount of information regarding the target domain in order to preserve the model's performance. Thus as an alternative way, prior studies have used transfer learning and domain adaptation techniques to effectively utilize labeled data from other subjects in combination with labeled data from the target subject, in order to compensate for limited availability of data from the target subject [25]–[27].

Taking a step further, unsupervised domain adaptation has

This work was supported by the Institute of Information and Communications Technology Planning and Evaluation (IITP) grant funded by the Korea government (MSIT) (No. 2017-0-00432). *(*Juho Lee and Jin Woo Choi contributed equally to this work.) (Corresponding author: Sungho Jo)*

Juho Lee was with the School of Computing, Korea Advanced Institute of Science and Technology, Daejeon, South Korea. He is now with LG Electronics, Seoul, South Korea.

Jin Woo Choi was with the Information & Electronics Research Institute, Korea Advanced Institute of Science and Technology, Daejeon, South Korea. He is now with the Department of Neurology & Neurological Sciences, Stanford University School of Medicine, Stanford, CA, USA.

Sungho Jo is with the School of Computing, Korea Advanced Institute of Science and Technology, Daejeon, South Korea (e-mail: shjo@kaist.ac.kr).

recently gained attention for solving domain shifts, as it does not require data labels from the target domain. This approach has been successfully applied in various fields, such as semantic segmentation and gesture recognitions using electromyography (EMG) signals [28]–[30]. Similar to other fields where obtaining labeled data poses significant challenges, collecting labeled brain signals for different motor imagery also requires a substantial amount of repetitive tasks to be performed by the user. Such procedures can be time-consuming and labor-intensive to both users and experts, as it involves following or instructing specific tasks and carefully inspecting the brain signals associated with each motor imagery label. Taking it into account, previous studies have developed unsupervised domain adaptation methods for BCIs and applied them to session-to-session problems, showing its potential to address cross-subject issues as well. These previous instances include Conditional Adversarial Domain Adaptation Neural Network (CDAN) [31] and Dynamic Joint Domain Adaptation Network (DJDAN) [32], which uses a gradient reversal layer (GRL) to learn commonly elicited features while reducing data discrepancy. Such unsupervised methods were investigated with the goal of making the signal acquisition procedure for new BCI users a simple calibration process rather than data collection that involves multiple repetitive tasks.

When dealing with unsupervised domain adaptation using motor imagery data from multiple subjects, extracting informative features can become a much more complex issue [33]. This is due to the fact that subjects may not be equally reliable and their data distributions may also differ, while data labels for the target subject are not available [34], [35]. Hence, adjusting the influences of each source domain may be a fundamental component in multiple source domain adaptation for cross-subject classification. Thus, in this paper, we propose a selective multi-source domain adaptation network (Selective-MDA) that can perform domain adaptation by considering the domain from each source subject separately along with their importance. Our Selective-MDA consists of two major ideas: a multi-source domain adaptation approach and a source-selective method. In order to utilize EEG signals from multiple subjects, the proposed network considers multiple sets of domain classifiers where each domain classifier treats each individual source subject. Furthermore, we investigated the effect of our source-selective method by comparing the discrimination performance of selecting different numbers of source domains along with their discrepancy measures on each epoch. To validate our method, we compared the performance with existing MI models and investigated the change in accuracy for the number of selected source subjects.

II. Related Works

Domain adaptation techniques have recently been handled with deep learning for BCIs in order to further extract features that are relevant to motor imagery. In cases where domain shifts are observed between source and target domains, domain adaptations utilize informative features from source domains to reduce time consumption for calibration. One of the frequently used methods to apply domain adaptation to EEG signaling is adversarial learning, which employs a domain discriminator along with a feature extractor to learn both the features from the domain and the features for classification. One such example includes the bi-hemisphere domain adversarial neural network (BiDANN) from Li et al., which applied adversarial learning for EEG-based emotion recognition in order to enhance the generality of the model and improve subject-independent classification [36]. Previous studies have also utilized adversarial learning for motor imagery classification. Two of the representative works include CDAN and DJDAN, an aforementioned model for domain adaptation based motor imagery classification [31], [32]. To be specific, the CDAN model utilizes a densely connected ConvNet model to first extract high-level discriminative features from the EEG signal, and uses a domain discriminator as an adversarial with the motor imagery classifier to learn domain-invariant EEG features. Within this phase, GRL is applied in the discriminator to reverse the gradient during back-propagation by multiplying with a negative value, thereby minimizing the classifier model from learning EEG signals from domains. DJDAN, on the other hand, utilizes a feature extractor similar to Shallow ConvNet and uses two different discriminators: a global discriminator that discriminates domain features by classifying between source and target domains, and a local discriminator that behaves similarly to the global discriminator but uses an additional estimation of confidence levels from the motor imagery classification results. The aforementioned architectures are designed as a single-source domain adaptation format, where a single discriminator is used to learn domains from sources.

To consider data from multiple domains, recent studies in various other fields have used multiple source domain adaptation to learn features that are related to classification tasks and invariant to multiple domain shifts. For instance, Zhao et al. proposed multi-source domain adversarial networks (MDAN) for sentiment analysis and image classification, which perform domain adaptation by optimizing and learning task-adaptive generalization bounds [37]. Unlike other previous domain adaptation models that utilize gradient reversal with a domain discriminator that manages all source domains, MDAN architecture employs multiple domain discriminators where each discriminator represents a single domain label. As another example, work from Guo et al. developed a DistanceNet model for text classification, using distance measures that differentiate samples between different domains and applying the measure to the loss function [38].

In light of the effects of adversarial learning techniques for EEG signals and multiple source domain adaptation from various fields, the aim of our model is to apply multiple source domain adaptation for cross-subject motor imagery classification. Inspired by DJDAN and MDAN models, our Selective-MDA uses multiple domain discriminators with high-end EEG features from the ConvNet model. To select subjects whose domains showed better adaptation to those of the target subject, we further hypothesized that subjects with greater loss from the domain discriminator, which may imply that their domains are not distinguishable from the target domain, would reflect such an aspect. To explore our hypothesis, we

This article has been accepted for publication in IEEE Transactions on Cognitive and Developmental Systems. This is the author's version which has not been fully edited and content may change prior to final publication. Citation information: DOI 10.1109/TCDS.2023.3314351

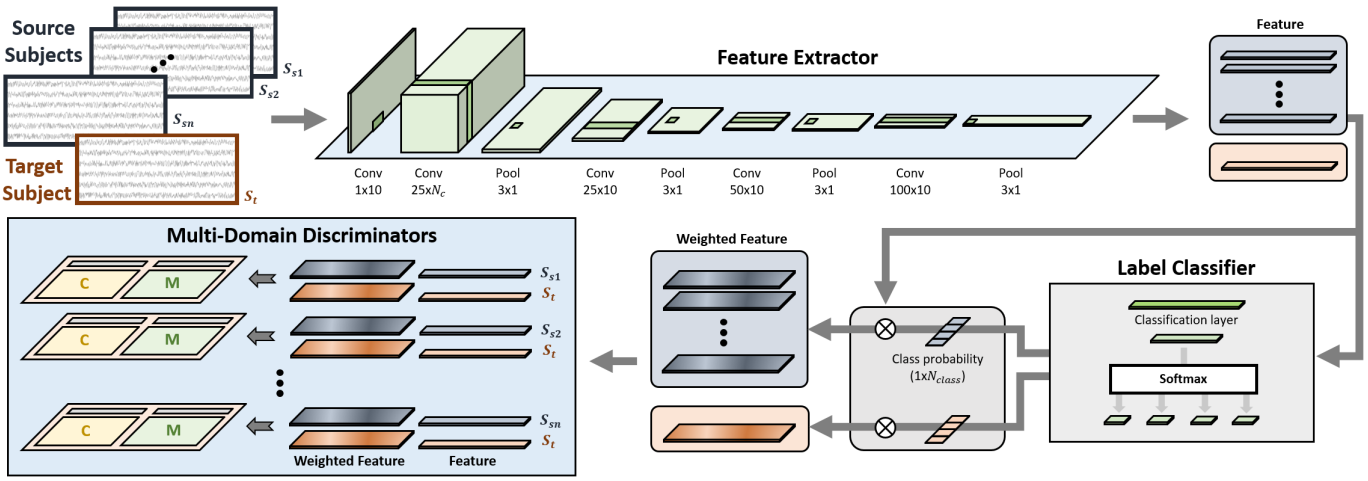

Fig. 1. The overall architecture of our Selective-MDA model. The model is composed of a feature extractor, a label classifier, and multi-domain discriminators. The sizes for the convolutional and pooling parameters used for the feature extractor are indicated on each layer.

investigated such matters by comparing results when selecting varying numbers of subjects as source domains based on the loss from the domain discriminator of each subject.

III. Methods

A. Definition and Notations

Suppose that the raw EEG data for training the model is denoted as $(x^T_{k,i}, y^T_{k,i})$, where x is EEG data from a training session T, k indicates a specific subject, and i represents a single EEG trial. A single EEG data from a trial is represented as $x^T_{k,i} \in \mathbb{R}^{N_c \times N_t}$, where N_c and N_t indicate the number of channels and time sampling points for EEG acquisition, respectively. The label from a trial is represented as $y^T_{k,i} \in \mathbb{R}^{N_l}$, where N_l indicates the number of total labels. As for our domain adaptation, we denote a source domain as $D_s = \{\{(x^T_{k,i}, y^T_{k,i})\}^{n_t}_{i=1}\}_{k \in S_s}$, where n_t is the number of EEG trials and S_s represents the set of subjects within the source domain. A target domain, which would be used for unsupervised adaptation, is denoted as $D_t = \{\{(x^E_{k,i}\}^{n_t}_{i=1}\}_{k \in S_t}$, where E is a symbol for the testing session of the EEG data and S_t represents the group of target subjects. Note that the target domain would only contain a single subject per single accuracy measure, therefore S_t would represent a group with a single subject value. Furthermore, label information from the target domain is not used to train the model.

B. Selective Multi-Source Domain Adaptation Architecture

The overall architecture of our Selective-MDA targeting for multiple source domain adaptation for EEG is shown in Figure 1. The architecture comprises three main components designed with inspiration from domain-adversarial training: a feature extractor, a label classifier, and multi-domain discriminators [39]. Our model first takes EEG signals as inputs and learns discriminant features with a feature extractor on both source and target domain data. The classifier of the model consecutively receives the extracted features and predicts the motor imagery label. Multi-domain discriminators, a set of domain discriminators assigned to each source-target pair, are followed after the classifier to determine whether the features belong to a source or target domain. Such a source-target pair design is utilized not only to address multiple source domains, but also to leverage their outcomes for our source selection approach. A gradient reversal layer is applied to each domain discriminator to prevent the extracted features from carrying discriminant information about the source or target domain. These overall components make the feature extractor extract domain-invariant features, making it difficult for the domain discriminators to determine whether the features are from the source or target domain [40].

1) Feature Extractor: The feature extractor in our model aims to learn class-discriminative features of each individual subject composing the source domains, extracting domain-invariant features for motor imagery. The feature extractor used for our model learns both oscillatory and spatial neural patterns by applying the Deep ConvNet structure, one of the widely used models for motor imagery classification [21]. Deep ConvNet hires a dense and deep architecture to contain a variety of features. Specifically, the input signal $x \in \mathbb{R}^{N_c \times N_t}$ for our model is first extracted into spatio-spectral features by going through a sequence of one-dimensional temporal and spatial convolutional layers. Followed by batch normalization, exponential linear unit (ELU) activation, max pooling and dropout, the features are further extracted while preventing overfitting. As deep ConvNet employs dense and deep architecture inspired by the field of computer vision, three additional blocks containing a convolutional layer, a batch normalization layer, an ELU activation, a max pooling layer, and a dropout layer are utilized to extract features of EEG data without overfitting. As we train both data from source and target domains to the feature extractor, feature representations from source and target domains noted as f^T and f^E are obtained as a result from x^T and x^E, respectively.

2) Classifier: The classifier model takes the output from the feature extractor as input. For both features from source and

This article has been accepted for publication in IEEE Transactions on Cognitive and Developmental Systems. This is the author's version which has not been fully edited and content may change prior to final publication. Citation information: DOI 10.1109/TCDS.2023.3314351

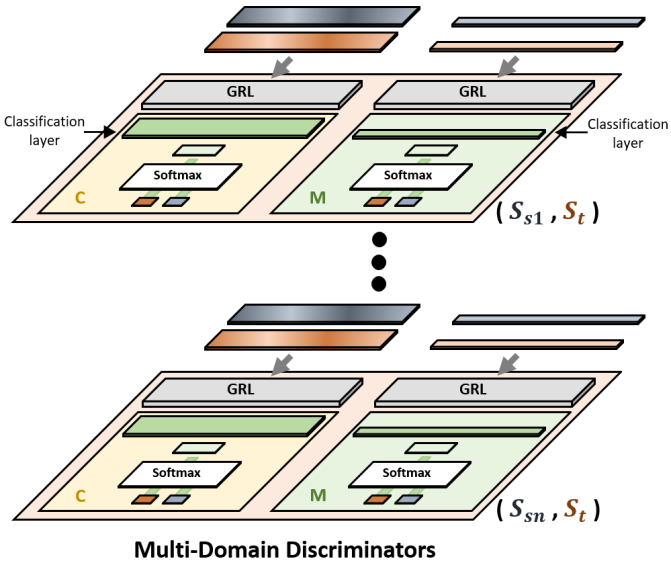

Fig. 2. The architecture of our multi-domain discriminators. Per a single source domain, a conditional discriminator and a marginal discriminator are employed to learn conditional and marginal domain-related classifiers that determine whether the extracted feature belongs to either source or target domain.

target domains f^T and f^E, a convolutional layer is applied for motor imagery label prediction. To be specific, a convolutional layer results in an output $p \in \mathbb{R}^{N_l}$ after softmax activation, where each cell represents the probability of the corresponding label. Thus, p^T and p^E are the output for source and target domains in the classifier.

As label information is required to train the classifier, data from target domains are not considered in calculating the loss function regarding the classifier. Thus, the loss for the classifier is measured with source domain information represented as follows:

$$L^k_{clf}(\theta_f, \theta_{clf}) = \mathbb{E}_{(x^T_{k,i}, y^T_{k,i}) \sim D_s} L(p^T_{k,i}, y^T_{k,i}) \quad (1)$$

where θ_f and θ_{clf} represent the model parameters for the feature extractor and classifier, respectively, k represents a specific subject, the function L indicates the cross-entropy loss function, and the indication $\mathbb{E}$ stands for the expected value. The number of calculated losses for classification is equal to the number of subjects forming the source domain.

3) Multi-domain Discriminators: As considering only the marginal distribution may still lead to discrepancies in the class-conditioned distribution [41], our model employs multi-domain discriminators that contain two different domain discriminator types for each single source domain: a marginal discriminator and a conditional discriminator, as shown in Figure 2. To be specific, a marginal discriminator takes in the extracted feature directly and the conditional discriminator uses a weighted feature computed from the extracted feature and the estimated label probability distribution. By considering conditional distribution alongside marginal distribution in the unsupervised domain adaptation, the model aims not only to align overall source and target distributions but also to align data from the same motor imagery class in the source and target domains considering the predicted labels from the classifier [32], [42]. Suppose that there is a total of k number of source domains, where each domain represents a single subject. There would thus be k number of the marginal discriminator and k conditional discriminators in the multi-domain discriminators.

The marginal discriminator accepts features from the feature extractor after going through a GRL, which makes the feature extractor learn domain-invariant features by inverting the gradient. The marginal discriminator is composed of a convolutional layer with softmax activation, which outputs two cells. The resulting two cells correspond to the probabilities of the feature being from the source and target domains, respectively. The loss of each marginal discriminator of a source domain is calculated as below:

$$L^k_{md}(\theta_f, \theta_{md}) = \mathbb{E}_{x^T_k \sim D_s} log[M_k(f^T_k)] - \mathbb{E}_{x^E_k \sim D_t} log[1 - M_k(f^E_k)] \quad (2)$$

where M_k corresponds to the marginal discriminator for the source domain k. Similar to the loss calculations from the classifier, the loss of the marginal discriminator is also measured for each source domain.

The conditional discriminator utilizes a refurbished feature represented by the product of the extracted features and the predicted probability. The conditional discriminator behaves similarly to the marginal discriminator, except for different inputs. The loss of each conditional discriminator of a subject within each label is therefore measured as follows:

$$L^{k,l}_{cd}(\theta_f, \theta_{cd}) = \mathbb{E}_{x^T_k \sim D_s} log[C_k(p^T_{k,l} \otimes f^T_k)] - \mathbb{E}_{x^E_k \sim D_t} log[1 - C_k(p^E_{k,l} \otimes f^E_k)] \quad (3)$$

where C_k corresponds to the conditional discriminator for a source domain k, and $p_{k,l}$ is the probability predicted by the classifier for label l from the source domain k. The refurbished features $p \otimes f$ embed discriminant information along with features by applying a product operation to the classifier results.

Both marginal and conditional domain distributions are considered using the above two types of discriminators. For multiple source adaptation, we applied two discriminators per source domain. Thus, the target domain was compared with each source domain, forming discriminators on an individual basis.

C. Source-Selective Method

Source subjects that are irrelevant or adversarial to the target subject may cause degradation of classification performance [43]. Recent studies in computer vision have addressed that considering the discrepancy of source and target domains by assigning weight or choosing source data that better align with the target domain may improve the model's performance [44], [45]. Taking such factors into account, our approach utilized a source-selective method that calculates the overall loss by selecting the source domains considered important at each epoch, as shown in Figure 3. The selection metric for our method prioritizes subject domains with higher conditional domain discriminator loss, which indicates that their learned

This article has been accepted for publication in IEEE Transactions on Cognitive and Developmental Systems. This is the author's version which has not been fully edited and content may change prior to final publication. Citation information: DOI 10.1109/TCDS.2023.3314351

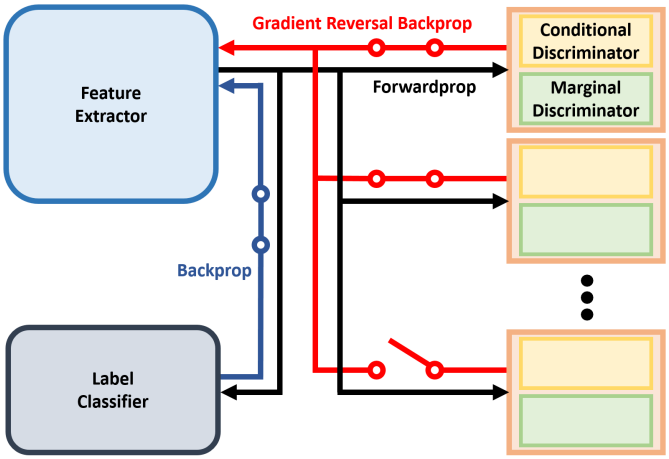

Fig. 3. A brief description regarding the source-selective method on Selective-MDA. The switches during backpropagation and gradient reversal backpropagation indicated in blue and red, respectively, are closed only on the selected subjects.

domain features are less distinguishable from the target domain, implying greater similarity between source and target distributions. While both marginal and conditional discriminators were used to align the distributions after selecting the source domains, the selection process was performed based on the conditional discriminator loss. With this approach, our model aims to select source domains that possess motor imagery class-conditioned distributions more similar to the target domain, which is in line with our primary objective of enhancing motor imagery classification performance.

Assuming that the number of subjects for source domain formation is N_s, then N_s number of subjects with the highest conditional discriminator loss from the previous training epoch are chosen to be considered as source domains. Thus, a set of selected source domains is defined as below:

$$S_{sub} = \underset{S' \subset S_s, |S'|=N_s}{argmax} \sum_{k \in S'} \sum_{l=1}^{N_l} L_{cd}^{k,l} \tag{4}$$

D. Optimization

Similar to the DJDAN model [32], we compute a dynamic adversarial factor ω of each selected source domain by employing the $\mathcal{H}$-distance for marginal and conditional distribution discrepancies with the following equations, respectively:

$$\begin{aligned} d_{k \in S_{sub}, \mathcal{H}, md}(D_k, D_t) &= 2(1 - 2\epsilon_m) \\ d_{k \in S_{sub}, \mathcal{H}, cd}(D_k, D_t) &= \frac{1}{N_l} \sum_{l=1}^{N_l} 2(1 - 2\epsilon_c^l) \end{aligned} \tag{5}$$

where ϵ_m represents the error rate from classification for the marginal discriminator, D_k indicates samples from a specific source domain k, and ϵ_c^l is the error rate for the conditional discriminator loss over the specific label l.

The ω of the selected source domains are therefore calculated with the following:

$$\omega_{k \in S_{sub}} = \frac{d_{k, \mathcal{H}, md}(D_k, D_t)}{d_{k, \mathcal{H}, md}(D_k, D_t) + d_{k, \mathcal{H}, cd}(D_k, D_t)} \tag{6}$$

As we have the loss values on each selected source domain from the classifier, the marginal discriminator, and the conditional discriminator, the final loss for a single source domain is therefore determined with the formula below:

$$L_{sub}^{k \in S_{sub}}(\theta_f, \theta_{clf}, \theta_{md}, \theta_{cd}) = \omega_k L_{md}^k + (1 - \omega_k) \sum_{l=1}^{N_l} L_{cd}^{k,l} \tag{7}$$

To further adapt the multiple numbers of domains selected for our model, we compute the overall loss of the model by using the following equation:

$$L_{overall} = \frac{1}{\gamma} log \sum_{k \in S_{sub}} exp(\gamma(L_{clf}^k - \alpha L_{sub}^k)) \tag{8}$$

where $\gamma > 0$ and $\alpha > 0$ are constants. Thus, the final loss for the model is measured by restraining losses from subjects neglected from domain selection. As our source selection method determines subjects with loss measures of the conditional discriminator from the previous epoch, source selection was not applied on the very first training epoch and all source subjects were used to formulate the source domains.

In order to learn domain-invariant features, the parameters of the feature extractor must be updated to predict the source subject's motor imagery label and not to distinguish domains. Thus, θ_f and θ_{clf} are trained to minimize the overall loss, and θ_{md} and θ_{cd} are trained to maximize the overall loss. Each parameter of the model is updated as below:

$$\begin{aligned} (\hat{\theta_f}, \hat{\theta_{clf}}) &= \underset{\theta_f, \theta_{clf}}{argmin}\ L(\theta_f, \theta_{clf}, \hat{\theta_{md}}, \hat{\theta_{cd}}) \\ (\hat{\theta_{md}}, \hat{\theta_{cd}}) &= \underset{\theta_{md}, \theta_{cd}}{argmax}\ L(\hat{\theta_f}, \hat{\theta_{clf}}, \theta_{md}, \theta_{cd}) \end{aligned} \tag{9}$$

Thus, the aim of the model is to train the feature extractor in such a way that the discriminators would be unable to classify whether the output feature is from the source or target domain.

IV. Experiments

A. Dataset

To evaluate our Selective-MDA, we used two public datasets widely used for motor imagery classification: Dataset IIa of BCI Competition IV [46] and Autocalibration and Recurrent Adaptation dataset [47].

1) Dataset IIa of BCI Competition IV: The dataset, which we will refer to as BCICIV, is acquired using 22 electrode EEG positions from a total of nine healthy participants. Each participant underwent two different experiment sessions held on different days. For each experiment session, participants were to perform one of the four motor imagery tasks depending on the visual cue, where the four motor imagery tasks included left hand, right hand, tongue, and feet movements. The signals were sampled at a 250 Hz frequency rate. Each motor imagery task was performed for 72 trials per experiment session. Of the two sessions from each participant, former session data from source subjects was used as training data representing the source domain, while the latter session data from the target subject was used as test data representing the target domain. Specifically for the four motor imagery classification, a total

of 576 trials per motor imagery from 8 source domains were used as a training dataset and 72 trials per motor imagery from a single target domain were used as a test dataset.

2) Autocalibration and Recurrent Adaptation Dataset: This dataset, which we will refer to as ARA, is retrieved using 13 electrode EEG positions from a total of 12 able-bodied, BCI-novice volunteers. At least two sessions were conducted for each participant, and one additional session was recorded for participants who did not reach the criterion level from the previous two sessions. We only used the first two sessions for our experiments. For each experimental session, participants were to perform one of the two motor imagery tasks, right hand and both feet movements, based on visual cues. The signals were sampled at a 512 Hz frequency rate. Each motor imagery task was performed for 100 trials per experiment session. We decided to use the first session of each participant as training data representing the source domain and the second session as test data representing the target domain. The third session was ignored. Thus with two motor imagery classification, 11 source domains from a total of 1100 trials per motor imagery were used as a training dataset, while a single target domain composed of 100 trials per motor imagery was used as a test dataset.

B. Signal Pre-processing

The datasets used were band-pass filtered from 4 to 38 Hz to include frequency band ranges relevant to motor imagery, taking into account previous studies [21], [32]. For each motor imagery trial, 0.5 seconds prior to the motor imagery cue to 4 seconds after the cue, corresponding to a 4.5-second EEG data per trial, was used for motor imagery data. In order to increase the data used for training and evaluation, each motor imagery trial was cropped with a 4-second sliding window with a stride of 0.5 seconds.

C. Experimental Models

In order to investigate the performance of our multi-source domain adaptation approach and our Selective-MDA, we compared the model performances with five different state-of-the-art deep learning models, where two of which include domain adaptation approaches on the architecture. Brief descriptions regarding the five models are noted as follows:

- Shallow ConvNet [21]: Inspired by the FBCSP algorithm, this model aims to strengthen discrimination by extracting features regarding oscillatory signals. The architecture of the model is comprised of temporal and spatial convolutional layers followed by a squaring non-linearity activation, an average pooling layer, and a logarithmic activation to formulate log-variance measurements from FBCSP.
- Deep ConvNet [21]: This model focuses on the depth of the model to extract a wider range of features. The architecture starts with oscillatory feature extraction with a convolutional layer. The architecture further consists of four blocks in a sequence composed of a convolutional layer and a max pooling layer, with batch normalization and exponential linear unit activation (ELU) in between. A dropout is applied lastly on all four blocks.
- EEGNet [22]: This model focuses on the compactness of the model to lessen the number of parameters to be trained. The model utilizes depth-wise and separable convolutional layers after temporal convolution to achieve compactness, and the ELU activation and average poolings are used to learn and merge spatial features corresponding to the spectral features.
- CDAN [31]: The model utilizes a domain adaptation method that aims to match conditional distribution between the source and target domains. The model consists of a feature extractor composed of a Dense ConvNet architecture followed by a classifier and a domain discriminator.
- DJDAN [32]: The model employs domain adaptation to adjust conditional and marginal distributions between the source and target domains. The model contains a Shallow ConvNet-based feature extractor, a classifier, and a domain discriminator that considers conditional and marginal features.

D. Evaluation

To first evaluate whether our multiple source domain adaptation architecture may enhance performance on motor imagery discrimination, we compared the accuracy of our Selective-MDA with the aforementioned state-of-the-art models. When measuring the accuracy, source and target domains were composed only with the dataset from training and testing sessions, respectively. The evaluation accuracy was measured with a leave-one-out cross-validation, where a single subject was used as a target domain while the remainders were used as source domains. Since there are 8 and 11 subjects for the source domain for the BCICIV and ARA datasets, respectively, we applied 8 and 11 different domain discriminators for comparison throughout epochs. Thus, source selection was not applied for comparison in the evaluation to explore the performance of the architecture itself.

TABLE I
ACCURACY COMPARISON WITH STATE-OF-THE-ART MODELS

Datasets	Models					
	Shallow	Deep	EEGNet	CDAN	DJDAN	Ours W/O Selection
BCICIV	43.33±11.34	44.08±14.19	41.96±13.44	44.91±9.96	46.39±13.07	**50.10±17.62**
ARA	61.85±8.89	64.02±8.97	64.44±9.64	63.54±7.60	64.92±9.80	**66.85±11.31**

This article has been accepted for publication in IEEE Transactions on Cognitive and Developmental Systems. This is the author's version which has not been fully edited and content may change prior to final publication. Citation information: DOI 10.1109/TCDS.2023.3314351

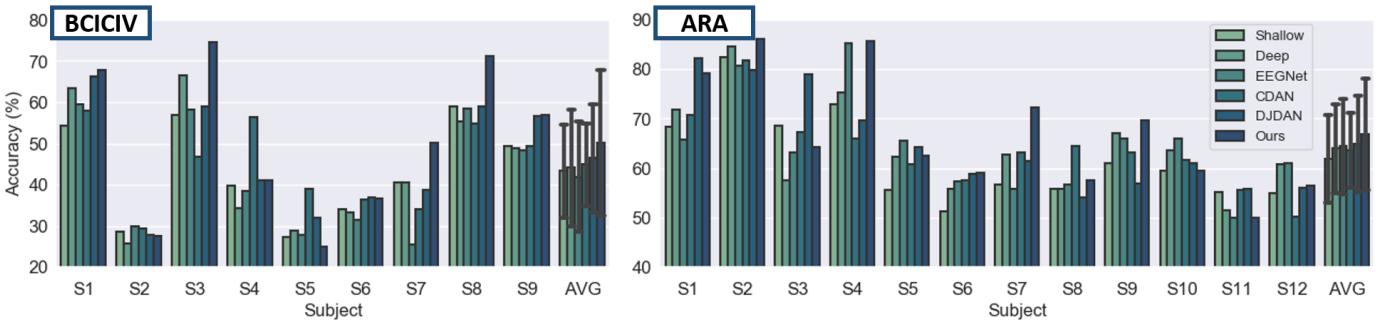

Fig. 4. Bar plots showing the classification accuracy of each model for all subjects. The left plot is the result for the BCICIV dataset, and the right plot is for the ARA dataset. The accuracy of our model refers to our multi-domain adaptation network without source selection. The error-bars refer to the standard deviation of the accuracies.

To further investigate our hypothesis that source selections based on domain similarity may improve cross-subject classification, we further evaluated the accuracy by taking a subset of source domains during loss measure via source selection. For each target domain, comparisons were made based on the selected number of source domains.

E. Experiment Settings

The proposed experiments were held within the Python framework, and the models were implemented with PyTorch. The models were trained on NVIDIA GeForce GTX 1080 Ti GPU with 11 GB Memory. An adaptive moment estimation (ADAM) optimizer was used to learn the model with a learning rate of 5e-4. In the case of CDAN, a stochastic gradient descent (SGD) optimizer was used as mentioned in the corresponding work. The used batch size varied between datasets, which were set to 64 and 32 for BCICIV and ARA, respectively. We also applied early stopping for our model after 3000 epochs, where the training stopped when the loss did not converge for over 20 consecutive epochs [48].

V. Results

A. Accuracy Comparison without Source Selection

The accuracy results of our multiple source domain adaptation model without our source selection method and the results of the state-of-the-art deep learning models are shown in Figure 4 and Table I for both BCICIV and ARA datasets. As shown in the figure and the table, the average accuracy was the highest when using our multiple source domain adaptation compared to the other five state-of-the-art models for the two datasets, despite the source selection method not being applied to the model. To be specific, our multi-domain adaptation network outperformed Shallow ConvNet, Deep ConvNet, EEGNet, CDAN and DJDAN with 50.10±17.62 for the BCICIV dataset (43.33±11.34, 44.08±14.19, 41.96±13.44, 44.91±9.96 and 46.39±13.07 for Shallow ConvNet, Deep ConvNet, EEGNet, CDAN and DJDAN respectively). As for the ARA dataset, our model also showed greater average accuracy with 66.85±11.31, whereas Shallow ConvNet, Deep ConvNet, EEGNet, CDAN and DJDAN exhibited the average accuracy of 61.85±8.89, 64.02±8.97, 64.44±9.64, 63.54±7.60 and 64.92±9.80 respectively. Furthermore, the accuracy results of each individual participant showed that our domain adaptation model without source selection outperformed the rest of the models on five out of nine subjects for the BCICIV dataset and five out of twelve for the ARA dataset. CDAN and DJDAN had the greatest accuracy on two subjects for BCICIV and four subjects for ARA, respectively, which were the next models after our architecture without source selection.

B. Accuracy Comparison with Source Selection

Table II and Table III show the accuracy results of subjects when different numbers of source domains were considered for the loss measure of each epoch for BCICIV and ARA datasets, respectively, with values in bold indicating the maximum accuracy exhibited from each subject. As for the BCICIV

TABLE II
Motor Imagery Classification Accuracy Results with Source Selection for BCICIV Dataset

# Sources	Subjects									AVG Accuracy
	S1	S2	S3	S4	S5	S6	S7	S8	S9	
1	59.20	28.65	61.81	36.81	24.65	26.39	46.53	62.85	40.45	43.04±14.48
2	66.84	27.26	66.84	42.36	26.39	30.21	**60.07**	66.15	48.61	48.30±16.43
3	63.54	26.22	63.89	39.58	**33.33**	38.02	59.38	70.49	55.21	49.96±14.93
4	68.75	25.35	68.06	47.74	30.38	35.94	59.20	**75.35**	56.25	**51.89±17.02**
5	69.97	27.78	66.67	**49.83**	25.00	**38.37**	53.65	72.22	**60.93**	51.60±16.78
6	**74.65**	27.60	62.67	45.31	27.08	36.11	44.27	70.31	58.68	49.63±16.77
7	70.66	**30.03**	66.32	43.23	25.00	36.81	53.65	70.14	58.68	50.50±16.43
8	67.71	27.60	**74.48**	41.15	25.00	36.63	50.17	71.18	56.94	50.10±17.62

This article has been accepted for publication in IEEE Transactions on Cognitive and Developmental Systems. This is the author's version which has not been fully edited and content may change prior to final publication. Citation information: DOI 10.1109/TCDS.2023.3314351

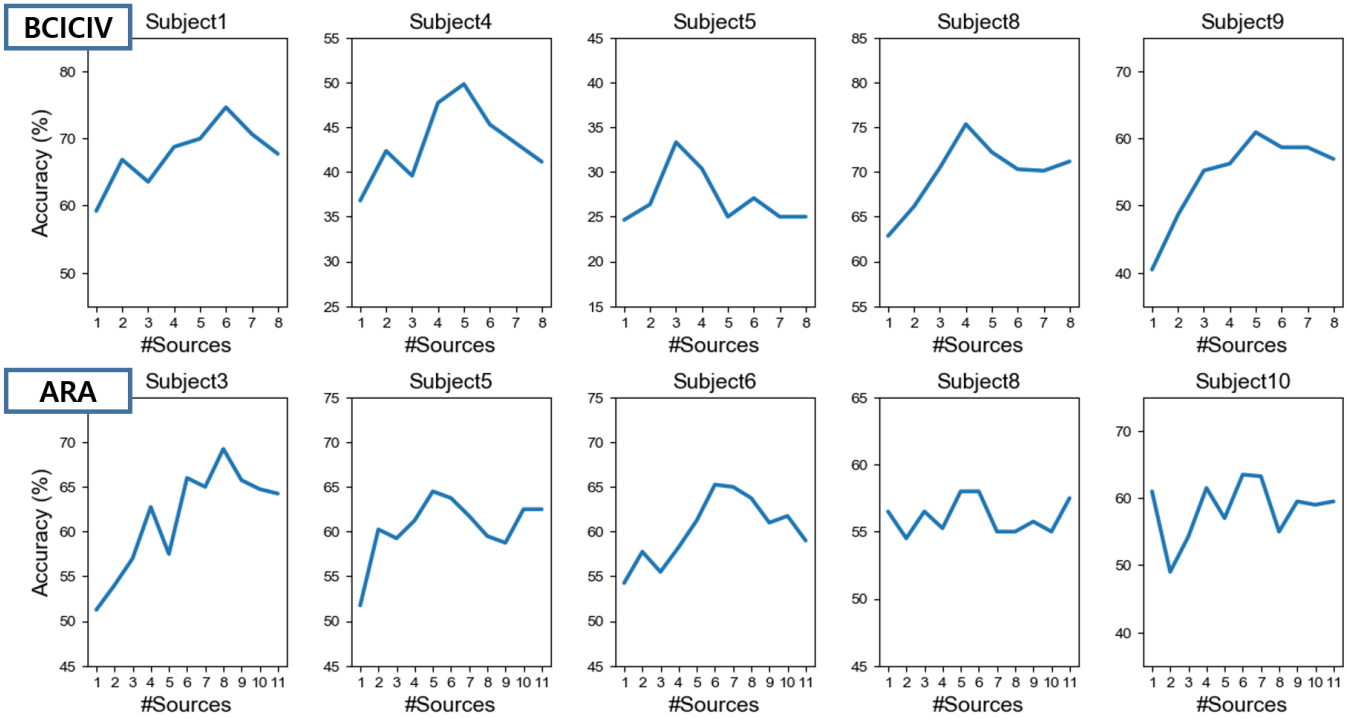

Fig. 5. Representative plots on the difference in accuracy when different numbers of sources were considered on each epoch for our Selective-MDA.

dataset, the results indicate that limiting the number of source domains to be used for loss calculation further improved the performance of the model, with eight out of nine subjects showing further improvement compared to when all subjects were continuously used to measure the loss on each epoch. Also for the ARA dataset, nine out of twelve subjects exhibited further improvement in their accuracy when source selection was used to limit the number of source domains to be considered for the loss calculation on each epoch.

The average accuracy of subjects was also analyzed to explore limiting the number of source domains of our Selective-MDA to which extent may provide the best model performance on the two used datasets. As can be seen from both Table II and Table III, the change in the average accuracy with respect to the number of source domains used for the loss measure of each epoch exhibited similar patterns on the two datasets. In the case of the BCICIV dataset from Table II, the average accuracy improved when more source domains were considered until it peaked at around half of the total source subjects (when 4 sources were considered on each epoch, average accuracy of 51.89±17.02), and showed a slight decrease thereafter with average accuracy not exceeding the former peak accuracy. Similarly for the ARA dataset from Table III, the average accuracy showed its improvement until half of the total source subjects (when 6 sources were considered on each epoch, average accuracy of 67.04±11.29), and did not further improve when more source domains were considered. Using the source selective method while limiting the number of considered sources to half of the total number of source domains on each epoch had the best average accuracy on both datasets, additionally improving the performance of our multi-source domain adaptation with 1.79 and 0.19 average

TABLE III
MOTOR IMAGERY CLASSIFICATION ACCURACY RESULTS WITH SOURCE SELECTION FOR ARA DATASET

# Sources	Subjects												AVG Accuracy
	S1	S2	S3	S4	S5	S6	S7	S8	S9	S10	S11	S12	
1	62.25	58.25	51.25	79.5	51.75	54.25	56.25	56.50	54.00	61.00	49.25	51.50	57.15±7.74
2	**88.50**	79.50	54.00	82.75	60.25	57.75	72.00	54.50	64.75	49.00	50.00	52.00	63.75±13.12
3	74.00	86.00	57.00	79.25	59.25	55.50	72.00	56.50	60.50	54.25	**57.50**	55.00	63.90±10.45
4	73.75	**88.50**	62.75	84.00	61.25	58.25	68.00	55.25	55.75	61.50	50.00	52.50	64.29±11.66
5	78.50	85.00	57.50	84.00	**64.50**	61.25	69.25	**58.00**	57.50	57.00	50.50	53.75	64.73±11.32
6	80.25	83.50	66.00	**88.50**	63.75	**65.25**	71.75	**58.00**	58.50	**63.50**	50.50	55.00	**67.04±11.29**
7	78.00	84.50	65.00	87.75	61.75	65.00	72.00	55.00	54.75	63.25	50.50	54.00	65.96±11.74
8	77.50	85.50	**69.25**	85.25	59.50	63.75	70.25	55.00	57.25	55.00	51.50	52.75	65.21±11.75
9	74.50	85.25	65.75	84.00	58.75	61.00	70.50	55.75	59.75	59.50	50.75	52.00	64.79±11.04
10	76.00	85.50	64.75	85.00	62.50	61.75	71.25	55.00	60.75	59.00	50.25	53.25	65.42±11.20
11	79.25	86.00	64.25	85.75	62.50	59.00	**72.25**	57.50	**69.75**	59.50	50.00	**56.50**	66.85±11.31

accuracy increase for BCICIV and ARA datasets, respectively. Moreover, when considering only the best accuracy from each subject, which represents the case where an optimized number for source selection was set individually on each subject, the average accuracy enhanced up to 55.23±17.12 and 70.17±11.58 for BCICIV and ARA datasets, respectively, showing 5.13 and 3.32 accuracy improvements compared to when no source selection was used.

VI. Discussion

The aim of our Selective-MDA is to extract domain-invariant motor imagery-related features with the data from multiple subjects. To prevent the feature extractor from learning domain-related features, we applied a multi-source domain adaptation technique where two different domain discriminators were applied per each source subject. With two major components of our study being 1) utilization of multi-source domain adaptation where each individual source domain is separately matched with the target domain and 2) application of our source selection method that further limits the influence of the data from the source domain which our model considered unreliable, we analyzed and compared our model with other state-of-the-art models in a two-step manner. The results from our experiment showed that even without our source selective method, our multiple-source domain adaptation approach was able to outperform other existing models both from average accuracy and from individual accuracy analysis. The performance was further improved by additionally applying our source selective method, which limits the number of source domains for measuring loss on each epoch. Specifically, the accuracy of subjects showed its greatest when the number of source domains selected was nearly half the number of total subjects, as can be seen in both used datasets (Figure 5). With the improved accuracy when limiting the number of source domains for loss calculation, our source selective domain adaptation approach was able to further enhance our multi-source domain adaptation architecture.

To explore whether the feature extractors were able to extract more discriminant motor imagery features when using our Selective-MDA network, we investigated the effect of source selection with visualization using t-SNE [49]. As seen in Figure 6 with the feature data of S8 and S6 as a representative plot for BCICIV and ARA datasets, respectively, the distribution of features was more discriminant within each motor imagery task when the multi-source domain adaptations were used without our selection method, compared to when no domain adaptation was used. The feature distribution showed further improvement when the selection method was further applied, resulting in better discriminant feature distribution compared to using the multi-source domain adaptation without our selective method. Such results indicate that the multi-domain discriminator of our model not only has supported feature extractors to better extract discriminant features using domain adaptation with gradient reversals, but also has prevented itself from over-trusting the source domains by utilizing our selective source method. Especially for classifying intentions with bio-signals such as EEG, our results indicate that using all source domains may not always be beneficial as seen in our study.

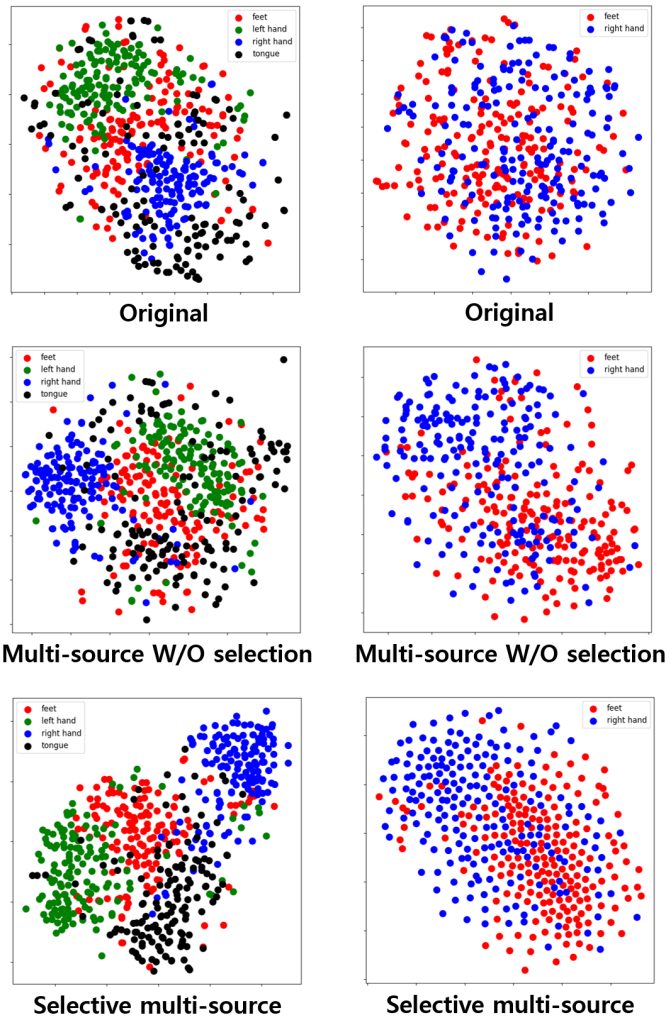

Fig. 6. Examples of t-SNE visualization from feature extractor on subject S8 (BCICIV) and subject S6 (ARA). Original represents feature distribution from Deep ConvNet, which can be referred to as our model without any domain discriminators.

The average confusion matrix results in Figure 7 show that our multiple-source domain adaptation techniques adjust feature extractors to learn features more evenly through each label. From the results of the BCICIV dataset seen in Figure 7, the overall accuracy of classifying all four motor imagery improved when using all source domains compared to when the domain adaptation was not applied, with the accuracy on each task being more evenly distributed. Such results indicate that while using no domain adaptation techniques may produce more biased features towards certain motor imagery tasks, using multiple source adaptations may lessen such bias occurrences. Furthermore from the results of applying our source selective domain adaptations, the accuracy results for all motor imagery tasks were enhanced compared to when using both cases of when all source domains were utilized or no domain adaptations were performed throughout learning. As shown in the results of our study, source-selective domain adaptation may lessen bias by preventing domain-wise features

This article has been accepted for publication in IEEE Transactions on Cognitive and Developmental Systems. This is the author's version which has not been fully edited and content may change prior to final publication. Citation information: DOI 10.1109/TCDS.2023.3314351

Fig. 7. A confusion matrix indicating grand average accuracy results for having each subject evaluated as a target domain. The results of when no source subject was used for domain adaptation, using all subjects for loss measure of our domain adaptation, and using the optimal number of source subjects on each epoch for loss measure are presented. The upper plots represent the results from the BCICIV dataset, and the lower plots represent the results from the ARA dataset.

to be learned from the feature extractor.

Our study of EEG signals also showed a positive impact of domain adaptation using deep learning, in accordance with previous studies in computer vision. Work from Ganin et al. [39] showed that decreasing both the risk from the source domain and the $\mathcal{H}$-divergence between the source and target domains may possibly reduce the target risk in terms of domain adversarial learning [50]. The feature extractor for domain adversarial learning is thus trained in a way that label classification performance on the source domain improves while the discrimination between source and target domains become more confused, leading to the extraction of domain-invariant features. Additionally, recent studies suggest that using the information from domain discriminators to prioritize source data that is more aligned with the target domain can further enhance the performance of tasks involving recognition of digits, images, and objects [44], [45]. As the loss from the domain discriminator provides information regarding the discrepancy between the source and target domains' feature distributions [40], [51], [52], our approach for EEG data selects source domains that show higher conditional domain discriminator loss when paired with the target domain at each epoch. By selecting source domains that are more difficult for the domain discriminators to distinguish, Selective-MDA aims to consider the similarity in distribution between source and target domains. The effects of this approach can be observed in our results. Our multi-source domain adaptation improved cross-subject motor imagery classification accuracy on two EEG datasets, even without source selection, showing that utilizing the domain discriminator for each source-target pair enhances model performance. By limiting the number of source domains considered at each epoch, our source selection approach could further improve the classification accuracy of the model. The comparison of t-SNE visualizations also provided instances that Selective-MDA were able to have positive influence on the feature extractor by enhancing feature distributions. Despite the inconsistent nature of EEG signals between and within individuals due to various reasons such as participants' motor imagery performance or their ability to elicit discriminant brain signals, our Selective-MDA results show that the approach had a positive impact on the feature extractor by considering relevant source domains for the target domain.

There are existing limitations and future works to be held on our study. While our Selective-MDA shows that limiting the number of sources to be used on each epoch may enhance domain adaptation, the number of subjects to be limited for source domains vary depending on the target domain. Along with the aforementioned limitation found in our study, further improvements regarding the determination of the optimal number of source subjects on each target domain may be performed to strengthen the applicability of our proposed method. Our selective method can also be improved with other criteria rather than considering the relevancy of each subject. In contrast to our model where a source domain represents its corresponding subject, other unit measures such as per trial or per task basis may be more suitable for source domain composition. As motor imagery performances may

even vary within individuals, additional studies investigating various compositions regarding source domains for our selection method may be held. Optimization of the network volume from the domain discriminators may also serve as one of the future works to be considered. The domain discriminator of our model is only used during model training aiming for the feature extractor to learn domain-invariant features, and the discriminators would not be used during its actual usage meaning that the corresponding volume would not be used during the testing phase. However, further attempts to lessen the volume while preserving its effect may be helpful, as it may lessen computation cost for model training. Lastly, future attempts on improving our model architecture may be carried out in advance. While our method determines the relevance of a source domain mainly with the loss of the domain discriminator, further consideration of other parameters or additionally learning the correlations between the domains may possibly improve the performance of the model.

VII. Conclusion

In this paper, we propose a selective multi-source domain adaptation network that performs unsupervised domain adaptation on each and every source subjects, and selectively limits their influences by restraining source domains with higher discrepancies from loss measure on each epoch. The results show that our proposed method of applying multiple domain discriminators, where each domain discriminator learns the domain features of each individual, improves classification accuracy as well as the extraction of discriminant motor imagery features. The source selection mechanism showed further improvements when applied to our multi-source domain adaptation in the aforementioned aspects, presenting its effectiveness for cross-subject motor imagery discrimination when multiple subjects were used as source domains. With the selective multi-source domain adaptation method in our study, we believe that EEG data from other subjects may also be harmoniously learned to extract motor imagery discriminant features, increasing the amount of training data that can be learned for the motor imagery classification model.

References

[1] G. Pfurtscheller and F. L. Da Silva, "Event-related eeg/meg synchronization and desynchronization: basic principles," *Clinical neurophysiology*, vol. 110, no. 11, pp. 1842–1857, 1999.

[2] Y. Liu, W. Su, Z. Li, G. Shi, X. Chu, Y. Kang, and W. Shang, "Motor-imagery-based teleoperation of a dual-arm robot performing manipulation tasks," *IEEE Transactions on Cognitive and Developmental Systems*, vol. 11, no. 3, pp. 414–424, 2018.

[3] M. Grosse-Wentrup and M. Buss, "Multiclass common spatial patterns and information theoretic feature extraction," *IEEE transactions on Biomedical Engineering*, vol. 55, no. 8, pp. 1991–2000, 2008.

[4] F. Lotte, L. Bougrain, A. Cichocki, M. Clerc, M. Congedo, A. Rakotomamonjy, and F. Yger, "A review of classification algorithms for eeg-based brain–computer interfaces: a 10 year update," *Journal of neural engineering*, vol. 15, no. 3, p. 031005, 2018.

[5] J. W. Choi, S. Huh, and S. Jo, "Improving performance in motor imagery bci-based control applications via virtually embodied feedback," *Computers in Biology and Medicine*, vol. 127, p. 104079, 2020.

[6] L. J. Greenfield, J. D. Geyer, and P. R. Carney, *Reading EEGs: A practical approach*. Lippincott Williams & Wilkins, 2012.

[7] L. Tonin, T. Carlson, R. Leeb, and J. d. R. Millán, "Brain-controlled telepresence robot by motor-disabled people," in *2011 Annual International Conference of the IEEE Engineering in Medicine and Biology Society*, pp. 4227–4230, IEEE, 2011.

[8] J. Jin, Z. Chen, R. Xu, Y. Miao, X. Wang, and T.-P. Jung, "Developing a novel tactile p300 brain-computer interface with a cheeks-stim paradigm," *IEEE Transactions on Biomedical Engineering*, vol. 67, no. 9, pp. 2585–2593, 2020.

[9] N. Kaongoen and S. Jo, "A novel hybrid auditory bci paradigm combining assr and p300," *Journal of neuroscience methods*, vol. 279, pp. 44–51, 2017.

[10] M. Middendorf, G. McMillan, G. Calhoun, and K. S. Jones, "Brain-computer interfaces based on the steady-state visual-evoked response," *IEEE transactions on rehabilitation engineering*, vol. 8, no. 2, pp. 211–214, 2000.

[11] P. Autthasan, X. Du, J. Arnin, S. Lamyai, M. Perera, S. Itthipuripat, T. Yagi, P. Manoonpong, and T. Wilaiprasitporn, "A single-channel consumer-grade eeg device for brain–computer interface: Enhancing detection of ssvep and its amplitude modulation," *IEEE Sensors Journal*, vol. 20, no. 6, pp. 3366–3378, 2019.

[12] G. Pfurtscheller and C. Neuper, "Motor imagery activates primary sensorimotor area in humans," *Neuroscience letters*, vol. 239, no. 2-3, pp. 65–68, 1997.

[13] J. W. Choi, B. H. Kim, S. Huh, and S. Jo, "Observing actions through immersive virtual reality enhances motor imagery training," *IEEE Transactions on Neural Systems and Rehabilitation Engineering*, vol. 28, no. 7, pp. 1614–1622, 2020.

[14] M. T. Sadiq, X. Yu, Z. Yuan, M. Z. Aziz, S. Siuly, and W. Ding, "A matrix determinant feature extraction approach for decoding motor and mental imagery eeg in subject specific tasks," *IEEE Transactions on Cognitive and Developmental Systems*, 2020.

[15] B. H. Yang, T. Wu, Q. Wang, and Z. J. Han, "Motor imagery eeg recognition based on wpd-csp and kf-svm in brain computer interfaces," in *Applied Mechanics and Materials*, vol. 556, pp. 2829–2833, Trans Tech Publ, 2014.

[16] M. Bentlemsan, E.-T. Zemouri, D. Bouchaffra, B. Yahya-Zoubir, and K. Ferroudji, "Random forest and filter bank common spatial patterns for eeg-based motor imagery classification," in *2014 5th International conference on intelligent systems, modelling and simulation*, pp. 235–238, IEEE, 2014.

[17] K. K. Ang, Z. Y. Chin, C. Wang, C. Guan, and H. Zhang, "Filter bank common spatial pattern algorithm on bci competition iv datasets 2a and 2b," *Frontiers in neuroscience*, vol. 6, p. 39, 2012.

[18] R. Zhang, Q. Zong, L. Dou, and X. Zhao, "A novel hybrid deep learning scheme for four-class motor imagery classification," *Journal of neural engineering*, vol. 16, no. 6, p. 066004, 2019.

[19] S. U. Amin, M. Alsulaiman, G. Muhammad, M. A. Bencherif, and M. S. Hossain, "Multilevel weighted feature fusion using convolutional neural networks for eeg motor imagery classification," *IEEE Access*, vol. 7, pp. 18940–18950, 2019.

[20] G. Dai, J. Zhou, J. Huang, and N. Wang, "Hs-cnn: a cnn with hybrid convolution scale for eeg motor imagery classification," *Journal of neural engineering*, vol. 17, no. 1, p. 016025, 2020.

[21] R. T. Schirrmeister, J. T. Springenberg, L. D. J. Fiederer, M. Glasstetter, K. Eggensperger, M. Tangermann, F. Hutter, W. Burgard, and T. Ball, "Deep learning with convolutional neural networks for eeg decoding and visualization," *Human brain mapping*, vol. 38, no. 11, pp. 5391–5420, 2017.

[22] V. J. Lawhern, A. J. Solon, N. R. Waytowich, S. M. Gordon, C. P. Hung, and B. J. Lance, "Eegnet: a compact convolutional neural network for eeg-based brain–computer interfaces," *Journal of neural engineering*, vol. 15, no. 5, p. 056013, 2018.

[23] W. Hang, W. Feng, R. Du, S. Liang, Y. Chen, Q. Wang, and X. Liu, "Cross-subject eeg signal recognition using deep domain adaptation network," *IEEE Access*, vol. 7, pp. 128273–128282, 2019.

[24] M. Riyad, M. Khalil, and A. Adib, "Cross-subject eeg signal classification with deep neural networks applied to motor imagery," in *Mobile, Secure, and Programmable Networking: 5th International Conference, MSPN 2019, Mohammedia, Morocco, April 23–24, 2019, Revised Selected Papers 5*, pp. 124–139, Springer, 2019.

[25] Y. Xu, Q. Wei, H. Zhang, R. Hu, J. Liu, J. Hua, and F. Guo, "Transfer learning based on regularized common spatial patterns using cosine similarities of spatial filters for motor-imagery bci," *Journal of Circuits, Systems and Computers*, vol. 28, no. 07, p. 1950123, 2019.

[26] M. Zheng, B. Yang, and Y. Xie, "Eeg classification across sessions and across subjects through transfer learning in motor imagery-based

brain-machine interface system," *Medical & biological engineering & computing*, vol. 58, no. 7, pp. 1515–1528, 2020.

[27] H. Zhao, Q. Zheng, K. Ma, H. Li, and Y. Zheng, "Deep representation-based domain adaptation for nonstationary eeg classification," *IEEE Transactions on Neural Networks and Learning Systems*, vol. 32, no. 2, pp. 535–545, 2020.

[28] M. Toldo, A. Maracani, U. Michieli, and P. Zanuttigh, "Unsupervised domain adaptation in semantic segmentation: a review," *Technologies*, vol. 8, no. 2, p. 35, 2020.

[29] U. Côté-Allard, G. Gagnon-Turcotte, A. Phinyomark, K. Glette, E. J. Scheme, F. Laviolette, and B. Gosselin, "Unsupervised domain adversarial self-calibration for electromyography-based gesture recognition," *IEEE Access*, vol. 8, pp. 177941–177955, 2020.

[30] P. P. Chan, Q. Li, Y. Fang, L. Xu, K. Li, H. Liu, and D. S. Yeung, "Unsupervised domain adaptation for gesture identification against electrode shift," *IEEE Transactions on Human-Machine Systems*, vol. 52, no. 6, pp. 1271–1280, 2022.

[31] X. Tang and X. Zhang, "Conditional adversarial domain adaptation neural network for motor imagery eeg decoding," *Entropy*, vol. 22, no. 1, p. 96, 2020.

[32] X. Hong, Q. Zheng, L. Liu, P. Chen, K. Ma, Z. Gao, and Y. Zheng, "Dynamic joint domain adaptation network for motor imagery classification," *IEEE Transactions on Neural Systems and Rehabilitation Engineering*, vol. 29, pp. 556–565, 2021.

[33] P. A. Abhang, B. W. Gawali, and S. C. Mehrotra, "Technological basics of eeg recording and operation of apparatus," *Introduction to EEG-and Speech-Based Emotion Recognition*, pp. 19–50, 2016.

[34] C. Guger, G. Edlinger, W. Harkam, I. Niedermayer, and G. Pfurtscheller, "How many people are able to operate an eeg-based brain-computer interface (bci)?," *IEEE transactions on neural systems and rehabilitation engineering*, vol. 11, no. 2, pp. 145–147, 2003.

[35] M. Ahn, H. Cho, S. Ahn, and S. C. Jun, "High theta and low alpha powers may be indicative of bci-illiteracy in motor imagery," *PloS one*, vol. 8, no. 11, p. e80886, 2013.

[36] Y. Li, W. Zheng, Y. Zong, Z. Cui, T. Zhang, and X. Zhou, "A bi-hemisphere domain adversarial neural network model for eeg emotion recognition," *IEEE Transactions on Affective Computing*, 2018.

[37] H. Zhao, S. Zhang, G. Wu, J. M. Moura, J. P. Costeira, and G. J. Gordon, "Adversarial multiple source domain adaptation," *Advances in neural information processing systems*, vol. 31, pp. 8559–8570, 2018.

[38] H. Guo, R. Pasunuru, and M. Bansal, "Multi-source domain adaptation for text classification via distancenet-bandits," in *Proceedings of the AAAI Conference on Artificial Intelligence*, vol. 34, pp. 7830–7838, 2020.

[39] Y. Ganin, E. Ustinova, H. Ajakan, P. Germain, H. Larochelle, F. Laviolette, M. Marchand, and V. Lempitsky, "Domain-adversarial training of neural networks," *The journal of machine learning research*, vol. 17, no. 1, pp. 2096–2030, 2016.

[40] Y. Ganin and V. Lempitsky, "Unsupervised domain adaptation by backpropagation," in *International conference on machine learning*, pp. 1180–1189, PMLR, 2015.

[41] A. Farahani, S. Voghoei, K. Rasheed, and H. R. Arabnia, "A brief review of domain adaptation," *Advances in data science and information engineering: proceedings from ICDATA 2020 and IKE 2020*, pp. 877–894, 2021.

[42] N. Lu, H. Xiao, Y. Sun, M. Han, and Y. Wang, "A new method for intelligent fault diagnosis of machines based on unsupervised domain adaptation," *Neurocomputing*, vol. 427, pp. 96–109, 2021.

[43] S. J. Pan and Q. Yang, "A survey on transfer learning," *IEEE Transactions on knowledge and data engineering*, vol. 22, no. 10, pp. 1345–1359, 2009.

[44] L. Yang, Y. Balaji, S.-N. Lim, and A. Shrivastava, "Curriculum manager for source selection in multi-source domain adaptation," in *Computer Vision–ECCV 2020: 16th European Conference, Glasgow, UK, August 23–28, 2020, Proceedings, Part XIV 16*, pp. 608–624, Springer, 2020.

[45] J. Zhang, Z. Ding, W. Li, and P. Ogunbona, "Importance weighted adversarial nets for partial domain adaptation," in *Proceedings of the IEEE conference on computer vision and pattern recognition*, pp. 8156–8164, 2018.

[46] C. Brunner, R. Leeb, G. Müller-Putz, A. Schlögl, and G. Pfurtscheller, "Bci competition 2008–graz data set a," *Institute for Knowledge Discovery (Laboratory of Brain-Computer Interfaces), Graz University of Technology*, vol. 16, pp. 1–6, 2008.

[47] J. Faller, C. Vidaurre, T. Solis-Escalante, C. Neuper, and R. Scherer, "Autocalibration and recurrent adaptation: Towards a plug and play online erd-bci," *IEEE Transactions on Neural Systems and Rehabilitation Engineering*, vol. 20, no. 3, pp. 313–319, 2012.

[48] R. Caruana, S. Lawrence, and L. Giles, "Overfitting in neural nets: Backpropagation, conjugate gradient, and early stopping," *Advances in neural information processing systems*, pp. 402–408, 2001.

[49] J. Donahue, Y. Jia, O. Vinyals, J. Hoffman, N. Zhang, E. Tzeng, and T. Darrell, "Decaf: A deep convolutional activation feature for generic visual recognition," in *International conference on machine learning*, pp. 647–655, PMLR, 2014.

[50] S. Ben-David, J. Blitzer, K. Crammer, and F. Pereira, "Analysis of representations for domain adaptation," *Advances in neural information processing systems*, vol. 19, 2006.

[51] S. Ben-David, J. Blitzer, K. Crammer, A. Kulesza, F. Pereira, and J. W. Vaughan, "A theory of learning from different domains," *Machine learning*, vol. 79, no. 1, pp. 151–175, 2010.

[52] M. Long, Z. Cao, J. Wang, and M. I. Jordan, "Conditional adversarial domain adaptation," *Advances in neural information processing systems*, vol. 31, 2018.